

Optical spectroscopy of the metal-insulator transition in NdNiO₃

T. Katsufuji, Y. Okimoto, T. Arima, and Y. Tokura
Department of Physics, University of Tokyo, Tokyo 113, Japan

J. B. Torrance

IBM Research Division, Almaden Research Center, 650 Harry Road, San Jose, California 95120-6099

(Received 6 October 1994)

We report optical measurements of NdNiO₃ that undergoes a phase transition from a paramagnetic metal to an antiferromagnetic insulator at 200 K ($= T_c$). The opening of a charge gap is observed in the optical conductivity spectrum [$\sigma(\omega)$] below T_c , and the missing spectral weight is distributed over the energy region above 0.3 eV. The evolution of the gap below T_c is rather gradual with temperature, in contrast to sharp changes of lattice parameters and resistivity at T_c . Such a feature in the $\sigma(\omega)$ spectrum of NdNiO₃ is characteristic of a spin-density-wave (SDW) state, though the peak energy (~ 0.4 eV) of the $\sigma(\omega)$ spectrum is considerably larger than that predicted by a simple SDW theory. The effect of electron correlation is discussed on the basis of the $\sigma(\omega)$ spectra.

I. INTRODUCTION

A metal-insulator (MI) transition caused by a strong electron-correlation effect is characteristic of 3d transition-metal compounds and their critical changes of electronic structures and properties in the course of the MI transition have been of particular interest. Recently, a series of perovskite-type Ni oxide compounds, $R\text{NiO}_3$, has been extensively studied from this viewpoint.¹⁻⁵ This system is characterized by a marked change of transport and magnetic properties with variation of the rare-earth (R) site. With systematically varying R species and temperature, Torrance *et al.*¹ have clarified the whole electronic phase diagram, which is composed of three regimes: a paramagnetic metal, a paramagnetic insulator, and an antiferromagnetic insulator. Such a variation of the electronic phase has been attributed to the variation of the electronic bandwidth associated with change of Ni-O-Ni bond angle, which critically depends on the ionic radius of R .¹ Namely, with decreasing ionic radius, the Ni-O-Ni bond angle decreases, and with it the bandwidth.

According to the electronic phase diagram of $R\text{NiO}_3$,¹ some of the compounds ($R=\text{Pr}$, Nd , Sm , and Eu) undergo a metal-to-insulator transition with decreasing temperature. Concerning such a thermally induced phase transition, transport properties, lattice structures,² magnetic structures,³ and pressure effects^{4,5} were investigated experimentally, and interpreted in terms of the formation of a charge-transfer (CT) gap (an excitation gap from the oxygen 2p state to the upper Hubbard band derived from the Ni 3d state). However, little is known about the electronic structure of the $R\text{NiO}_3$ system and its change with the MI transition. To clarify this point, we have carried out optical measurements of NdNiO₃, as a typical compound of $R\text{NiO}_3$ that undergoes a MI transition with changes in temperature. The measure-

ments were made with carefully controlled temperature changes, which enabled us to provide a quantitative discussion about the temperature dependence of the electronic structure of this compound across its MI transition.

II. EXPERIMENT

The polycrystalline sample investigated in this study is the same one used in previous studies;¹ details are described in Ref. 1. According to the resistivity measurement and a muon-spin relaxation experiment,¹ the MI transition temperature (T_c) is nearly identical to the antiferromagnetic ordering temperature (T_N), 200 K.

Reflectivity measurements were performed using a Fourier-transform interferometer between 0.06 and 0.8 eV, and grating spectrometers between 0.6 and 36 eV. Synchrotron radiation at INS-SOR, University of Tokyo, was utilized for the measurements between 6 and 36 eV. To measure the temperature dependence of the reflectivity spectra, we mounted the crystal in a He cryostat, and carried out the measurement during heating between 0.06 and 3 eV. A gold mirror that was mechanically placed at the sample position within the cryostat was used as a reference. We also measured the reflectivity spectra at room temperature using a microscope spectrometer with half of the sample covered by evaporated Au as a reference. The reflectivity obtained by the latter method was discernibly larger than that obtained by the former method, particularly above 1 eV (approximately 1.5 times). This discrepancy is likely due to the light scattering off the sample surface (which is usually unavoidable in conventional reflectivity measurements of ceramic samples). Therefore, we corrected the spectra at all temperatures by multiplying them by the ratio of above-mentioned two reflectivity spectra at room temperature. Such a correction

involves some uncertainty in absolute reflectivity with varying temperature. However, as described below, the variation of reflectivity with temperature is large only below 0.5 eV, where the discrepancy by the two methods is not critical to the arguments.

Optical response functions were obtained by Kramers-Kronig analysis of the reflectivity data from 0.06 eV to 3 eV at each temperature and from 3 eV to 36 eV at room temperature. We have confirmed that extrapolation of reflectivity below 0.06 eV has a negligible effect on the derived spectra, and thus adopt constant extrapolation at all temperatures. Above 36 eV, extrapolation was made by using the ω^{-4} functional dependence.

III. RESULTS

Figure 1 shows the optical conductivity $[\sigma(\omega)]$ spectrum for NdNiO₃ up to 15 eV at room temperature. The $\sigma(\omega)$ spectrum was obtained by the Kramers-Kronig analysis of the reflectivity spectrum shown in the inset. A large peak around 10 eV is assigned to the transition from the oxygen 2*p* state to the Nd 5*d*/4*f* state, which is a commonly observed structure in transition metal oxides containing rare-earth atoms (including high T_c cuprates⁶). Below 5 eV, a nearly constant conductivity continues down to 1 eV, below which a Drude-like tail is observed. Arima *et al.*⁷ compared the $\sigma(\omega)$ spectra for LaMO₃ (M =transition metal) with calculated values of the charge-transfer (CT) excitation gap between the oxygen 2*p* state and the M 3*d* state. For M =Ni (LaNiO₃), they concluded that a nearly flat spectrum below 5 eV is due to the CT excitation whose spectral weight remains at $\omega = 0$ eV, which leads to the metallic state of LaNiO₃. Because of the similarity between the $\sigma(\omega)$

spectra for LaNiO₃ and NdNiO₃ at room temperature, the spectral weight below 5 eV (a shaded region in Fig. 1) is also attributable to CT excitations. Thus, conduction carriers of this compound, which are responsible for the Drude-like tail observed in the $\sigma(\omega)$ spectrum in Fig. 1, exhibit strongly hybridized characteristics involving Ni 3*d* and oxygen 2*p* states.

We show the temperature dependence of reflectivity spectra $R(\omega)$, optical conductivity $\sigma(\omega)$, and of the real part of dielectric constant $\epsilon_1(\omega)$ below 2 eV in Figs. 2(a), 2(b), and 2(c), respectively. At 290 K, the reflectivity gradually increases towards $\omega = 0$. In consonance with the reflectivity spectrum, an $\omega \sim 0$ peak for $\sigma(\omega)$ and a negative value of $\epsilon_1(\omega)$ in the low frequency region (< 0.6 eV) are clearly observed, both of which are characteristic of the optical response of metals. However, these spectra cannot be reproduced by the simple Drude form

$$\sigma(\omega) = \frac{ne^2}{m^*} \frac{\Gamma}{\omega^2 + \Gamma^2}, \quad (1)$$

$$\epsilon_1(\omega) = \epsilon_\infty - \frac{4\pi ne^2}{m^*} \frac{1}{\omega^2 + \Gamma^2}. \quad (2)$$

As an attempt to overcome this difficulty, we have analyzed these spectra in terms of ω -dependent scattering rate Γ and effective mass m^* (extended Drude model). In this analysis, one can obtain ω -dependent forms of m^* and Γ from the optical response function. Figure 3 shows the result, which indicates that both, m^* and Γ , depend on ω . In particular, Γ increases with ω , and exceeds ω itself over the whole energy range. This calls into question the applicability of the extended Drude model for metallic NdNiO₃, since $\Gamma(\omega)$ should be smaller than ω when one interprets transport properties in terms of the quasiparticle picture. However, such a non-Drude-like behavior is characteristic of metallic 3*d* electron transition metal oxide, such as high- T_c cuprates and LaTiO₃.⁸ Thus, the interpretation of the spectra remains an unsettled problem.

According to Fig. 2, $R(\omega)$, $\sigma(\omega)$, and $\epsilon_1(\omega)$ remain unchanged down to 207 K (just above T_c), which indicates that the electronic structure of this compound is essentially unchanged in the metallic phase. Below $T_c \sim 200$ K, a variation of the reflectivity is clearly observed, particularly as a large decrease below 0.5 eV. In consonance with this, the low-energy spectral weight in the $\sigma(\omega)$ spectra begins to decrease and the lost spectral weight appears to be redistributed over the higher energy region (> 0.3 eV). A gap structure also clearly develops. At the lowest temperature, i.e., 9 K, a drop in the $\sigma(\omega)$ spectrum sets in at ~ 0.4 eV, and the minimum gap energy, which is estimated by extrapolating the steeply decreasing part of the spectra to zero, is ~ 0.03 eV. A variation is also found in the $\epsilon_1(\omega)$ spectra below 200 K, where the sign of the low-frequency part (< 0.6 eV) changes from negative to positive. All these results are consistent with the phase transition from the metallic to the insulating state with a gap energy of ~ 200 K, which is consistent with the temperature dependence of the resistivity.¹

We plot in Fig. 4 temperature dependence of σ (closed circles) and ϵ_1 (open circles) at $\omega = 0.08$ eV (which is the

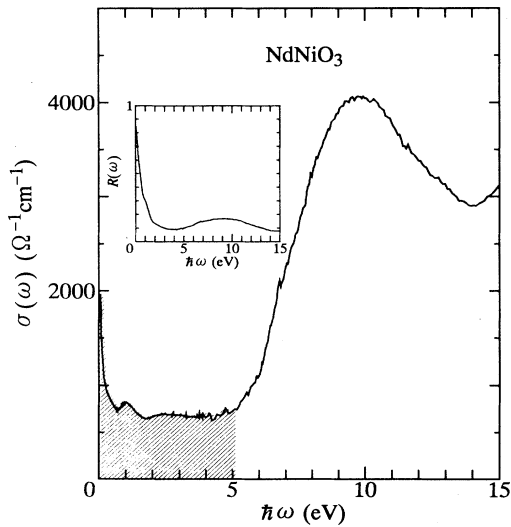


FIG. 1. The optical conductivity $[\sigma(\omega)]$ spectrum for NdNiO₃ up to 15 eV at room temperature. Shaded region refers to the excitation from oxygen 2*p* state to Ni 3*d* state. (see the text.) The inset shows the reflectivity spectrum at room temperature.

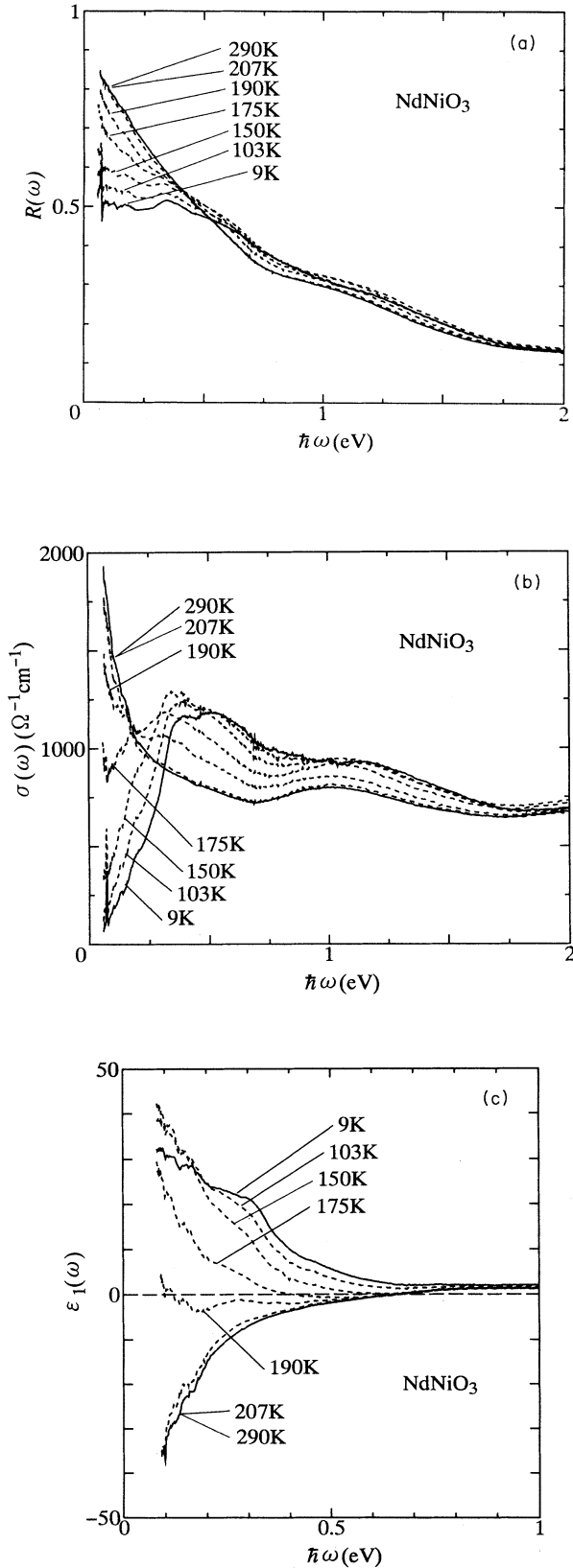


FIG. 2. Spectra for (a) reflectivity $R(\omega)$, (b) optical conductivity $\sigma(\omega)$, and (c) a real part of dielectric constant $\epsilon_1(\omega)$, for NdNiO_3 at various temperatures.

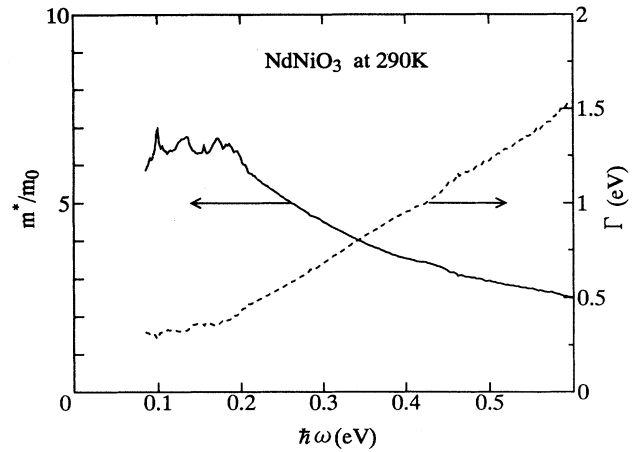


FIG. 3. ω dependence of effective mass (m^* normalized by the free electron mass m_0) and scattering rate (Γ) at room temperature, derived by the extended Drude model.

energy immediately above that of the highest-lying optical phonon). Both values show a critical change at 200 K: σ decreases and ϵ_1 increases with diminishing temperature. A large value of ϵ_1 (30–40) in the insulating phase also indicates a narrow gap feature for the insulating state.

For a more quantitative analysis of the temperature dependence of the electronic structure, we specified the effective number of electrons (N_{eff}) by

$$N_{\text{eff}}(\omega) = \frac{2m_0}{\pi e^2 N} \int_0^\omega \sigma(\omega') d\omega', \quad (3)$$

where m_0 is the free electron mass and N , the number of Ni atoms per unit volume. Equation (3) refers to the number of electrons that contribute to conduction below ω . Figure 5 shows the value of $N_{\text{eff}}(\omega_c = 0.3 \text{ eV})$ as a function of temperature (closed circles) in comparison

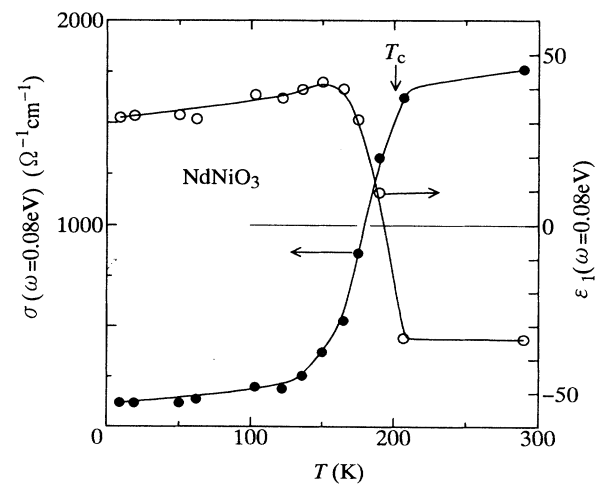


FIG. 4. Temperature dependence of optical conductivity (σ) and a real part of dielectric constant (ϵ_1) at 0.08 eV. Solid lines are the guide to eyes.

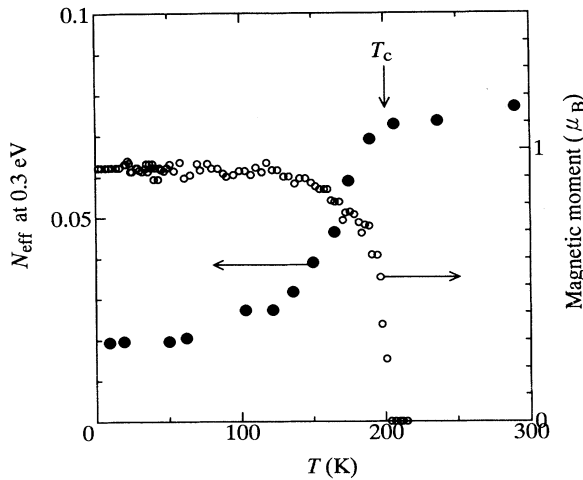


FIG. 5. Effective number of electrons (N_{eff}) at 0.3 eV (closed circles) and the magnetic moment obtained by a neutron scattering measurement (reproduced from Ref. 3; open circles) as a function of temperature.

with the magnetic moment measured by neutron scattering measurements.³ Here, the cutoff energy ($\omega_c = 0.3$ eV) corresponds to the energy of the intersection of the $\sigma(\omega)$ spectra at 290 K and 9 K, i.e., the center of the spectral weight transfer. N_{eff} does not change with temperature down to 200 K. Below 200 K, N_{eff} begins to decrease as a result of the gap formation associated with the MI transition, and keeps decreasing down to (at least) 100 K. The difference between N_{eff} at 290 K (a metallic phase) and that at 9 K (an insulating phase), ~ 0.058 , represents the spectral weight ($\sim 4\pi Ne^2/m^*$) that pertains to the conduction properties in the metallic phase. If we assume one conduction electron per Ni site, this value leads to an effective mass ratio $m^*/m_0 = 1/0.058 \sim 17$, where m^* is the effective mass of conduction carriers and m_0 the free-electron mass. Such a large value of m^*/m_0 is characteristic of the narrow conduction band composed of Ni 3d and O 2p levels, and of the mass enhancement by strong electron-correlation effects. Note that the electronic specific-heat coefficient (γ) for metallic LaNiO₃ (Ref. 9) is $\gamma \sim 13.8$ mJ/K²mol, which also indicates a large value of m^*/m_0 (~ 10 on the basis of the free electron model).

Even more striking in Fig. 5 is the rather gradual temperature dependence of N_{eff} below T_c , which is similar to the temperature dependence of the magnetic moment³ as shown in the same figure, and is quite in contrast with the sharp change of resistivity at T_c .¹ As described above, the measurement was carried out during a warming run; hence, a coexistence of the metallic phase and insulating phase below T_c (which actually occurs in a cooling run below T_c as reported in Ref. 10 for PrNiO₃) is very unlikely and cannot be the origin of the gradual change of N_{eff} . Thus, the temperature dependence of N_{eff} appears to be intrinsic for this compound. The MI transition, though being of first order at $T_c \sim 200$ K, is thus obviously dominated by a continual change of the electronic structure below T_c .

IV. DISCUSSION

One of the possible interpretations of the MI transition in NdNiO₃ at 200 K is to assign an active role to the lattice structure upon the transition. The lattice structure of NdNiO₃ was investigated as a function of temperature by neutron scattering measurements.² The lattice symmetry does not change at the MI transition, but the lattice parameters show an abrupt change in the narrow range (~ 10 K width) of temperature below T_c . These features are, however, in contrast with the temperature dependence of N_{eff} , whose change continues down to 100 K. This leads to the conclusion that changes in the lattice structure play merely a subsidiary role in the alteration of the electronic structure during the MI transition.

According to the electronic phase diagram of RNiO₃,¹ the MI transition of NdNiO₃ is accompanied by the simultaneous onset of antiferromagnetic ordering. This feature is similar to that encountered in PrNiO₃, but differs from that of SmNiO₃ or EuNiO₃, in which an MI transition occurs at temperatures higher than the magnetic ordering temperature. Accordingly, we may consider the magnetic ordering effects to be the origin of the MI transition for NdNiO₃. In this view, a spin-density-wave (SDW) gap is a candidate for the charge gap in the insulating phase of NdNiO₃. Properties of an SDW state were extensively studied for Cr metal, which undergoes an SDW transition at 312 K.¹¹ Optical measurements were also carried out for the SDW phase of Cr,¹² and a peak structure due to the excitation across the SDW gap was observed in the $\sigma(\omega)$ spectrum. Such a peak structure in the $\sigma(\omega)$ spectrum of the SDW state relates to the theoretical fact that $\sigma(\omega)$ diverges when $\omega \rightarrow 2\Delta$ (gap energy¹³). In other words, the missing spectral weight below the SDW gap is distributed immediately above the gap energy. Such a peak can be observed in the spectrum for NdNiO₃ at ~ 0.4 eV in the insulating phase as shown in Fig. 2, which is similar to that for Cr metal.

The value of the SDW gap energy is closely related to that of the ordered magnetic moment, and temperature dependence of both is given by the BCS gap function.¹⁴ In Fig. 6 we plot the temperature dependence of the $\sigma(\omega)$ spectra in the low-energy region (< 0.4 eV). One finds that the increasing part of $\sigma(\omega)$ shifts towards higher energies with decreasing temperature, which suggests an increase of the gap energy. The inset shows the temperature dependence of 2Δ , which is defined as the midpoint of the gaplike rise of $\sigma(\omega)$, i.e., the energy where $\sigma(\omega) = 600 \Omega^{-1}\text{cm}^{-1}$. The temperature dependence of this value is roughly in accord with the BCS gap function, as shown by the solid curve.

There are points that are not consistent with the conventional SDW state. First, the temperature dependence of the magnetic moment³ (see Fig. 5) is rather steep immediately below T_N , perhaps reflecting the first-order nature of the transition, and hence is not in good agreement with the SDW model,¹⁴ i.e., the BCS gap function. A more serious discrepancy is about the magnitude of the charge gap in the ground state, which is given also by the BCS gap function, $2\Delta(T=0) = 3.5k_B T_N$. For Cr metal, a modified theory that takes account of the scat-

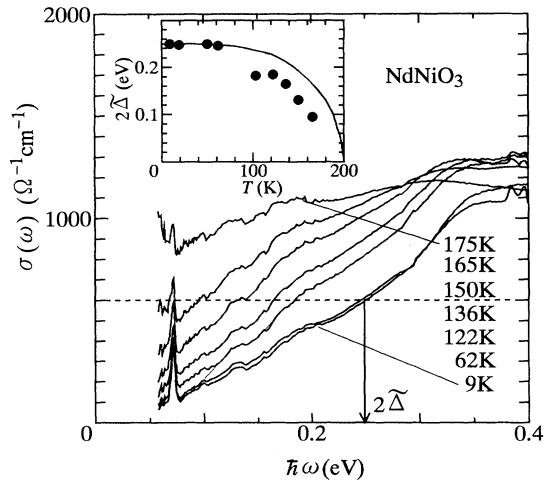


FIG. 6. Temperature dependence of $\sigma(\omega)$ spectra in the low-energy region (<0.4 eV). The inset shows the temperature dependence of $2\tilde{\Delta}$, the energy where $\sigma(\omega) = 600 \Omega^{-1}\text{cm}^{-1}$.

tering of electrons by phonons reproduces the experimentally observed peak energy, $5.2k_B T_N$. By contrast, the peak energy (0.4 eV) for NdNiO₃ at 9 K is $\sim 20k_B T_N$, which is considerably larger than the theoretically predicted value. Such a discrepancy was also observed for NiS,¹⁵ which is also classified as a strongly correlated electron system.

Up to now, several theoretical studies have been carried out based on the Hubbard Hamiltonian with the on-site Coulomb energy (U) and the transfer integral (t) (Refs. 16, 17) that reproduces an electronic phase diagram similar to that of $R\text{NiO}_3$.¹ According to these theories, a small- U region, where T_N increases with increasing U/t (i.e., decreasing t), is consistent with the weak coupling theory in the random phase approximation (RPA), and a large- U region, where T_N decreases with increasing U/t , is in terms of the Heisenberg spin Hamiltonian. In the $R\text{NiO}_3$ system, the decrease of ionic radius of R leads to the decrease of t , as described in Sec. I. Therefore, if the Hubbard-model picture is applied to the $R\text{NiO}_3$ family, PrNiO_3 and NdNiO_3 would fall in the weak coupling region, whereas those containing rare earth ions smaller than Nd fall in the strong coupling

region. In the strong coupling region with small R ions, the charge gap is dominated by the CT excitation gap Δ , in which the antiferromagnetic exchange interaction is given by $J = 2t_{pd}^4/\Delta^2(1/U_d + 1/\Delta)$ (Ref. 18), t_{pd} being the transfer integral between the Ni 3d state and the oxygen 2p state, and U the on-site Coulomb repulsion energy at a Ni 3d site. On the other hand, in the weak coupling region with relatively larger R ions, the antiferromagnetic state is similar to the SDW state; hence the charge gap is characteristic of the SDW gap. NdNiO₃ belongs to the weak-coupling region but may have an intermediate character as well, since it is located near the maximum of T_N in the phase diagram, i.e., close to the border of the two regions. This might be the origin of the observed deviation from the conventional SDW theory. To confirm this, a systematic experimental investigation of the charge gap in the $R\text{NiO}_3$ system (other than NdNiO₃) will be useful, which is now in progress.

V. SUMMARY

We measured reflectivity spectra with varying temperature for NdNiO₃, and derived response functions from the Kramers-Kronig analysis. We found that a charge gap opens up in the $\sigma(\omega)$ spectrum upon the MI transition at 200 K, and that the missing spectral weight below the gap is distributed over more 0.3 eV. The effective number of electrons [which measures the missing spectral weight and is defined as an ω integral of the $\sigma(\omega)$ spectrum up to 0.3 eV] shows rather gradual temperature dependence in contrast with the critical change of, for example, the lattice parameters at T_c . Such a temperature dependence of the charge-gap formation is qualitatively similar to the case of the SDW transition, though the value of the charge gap is larger than that predicted by the conventional SDW theory. This may be an indication that electron correlation effect should be taken into account more explicitly.

ACKNOWLEDGMENT

The present work was partly supported by a Grant-In-Aid for Scientific Research from Ministry of Education, Science, and Culture, Japan.

¹ J. B. Torrance, P. Lacorre, A. I. Nazzal, E. J. Ansaldo, and Ch. Niedermayer, Phys. Rev. B **45**, 8209 (1992).
² J. L. Garcia-Muñoz, J. Rodriguez-Carvajal, P. Lacorre, and J. B. Torrance, Phys. Rev. B **46**, 4414 (1992).
³ J. L. Garcia-Muñoz, J. Rodriguez-Carvajal, and P. Lacorre, Europhys. Lett. **20**, 241 (1992).
⁴ X. Obradors, L. M. Paulius, M. B. Maple, J. B. Torrance, A. I. Nazzal, J. Fontcuberta, and X. Granados, Phys. Rev. B **47**, 12353 (1993).
⁵ P. C. Canfield, J. D. Thompson, S-W. Cheong, and L. W. Rupp, Phys. Rev. B **47**, 12357 (1993).
⁶ S. Uchida, T. Ido, H. Takagi, T. Arima, Y. Tokura, and S.

Tajima, Phys. Rev. B **43**, 7942 (1991).

⁷ T. Arima, Y. Tokura, and J. B. Torrance, Phys. Rev. B **48**, 17006 (1993).

⁸ L. D. Rotter *et al.*, Phys. Rev. Lett. **67**, 2741 (1991); Y. Fujishima *et al.*, Phys. Rev. B **46**, 11167 (1992); D. A. Crandles *et al.*, *ibid.* **49**, 16207 (1994).

⁹ K. Sreedhar, J. M. Honig, M. Darwin, M. McElfresh, P. M. Shand, J. Xu, B. C. Crooker, and J. Spalek, Phys. Rev. B **46**, 6832 (1992).

¹⁰ X. Granados, J. Fontcuberta, X. Obradors, and J. B. Torrance, Phys. Rev. B **46**, 15683 (1992).

¹¹ C. Herring, in *Magnetism*, edited by G. T. Rado and H.

- Suhl (Academic Press, New York, 1967).
- ¹² A. S. Barker, Jr., B. I. Halperin, and T. M. Rice, Phys. Rev. Lett. **20**, 384 (1968).
- ¹³ P. A. Fedders and P. C. Martin, Phys. Rev. **143**, 245 (1966).
- ¹⁴ A. W. Overhauser, Phys. Rev. **128**, 1437 (1962).
- ¹⁵ A. S. Barker, Jr. and J. P. Remeika, Phys. Rev. B **10**, 987 (1974).
- ¹⁶ T. Moriya and H. Hasegawa, J. Phys. Soc. Jpn. **48**, 1490 (1980).
- ¹⁷ J. E. Hirsch, Phys. Rev. B **35**, 1851 (1987).
- ¹⁸ H. Matsukawa and H. Fukuyama, J. Phys. Soc. Jpn. **58**, 2845 (1989).